Super-localization of contrast agents in moving organs, first experiments in a rat kidney

Josquin Foiret, Hua Zhang, Lisa Mahakian, Sarah Tam, Katherine W. Ferrara
Department of Biomedical Engineering,
UC Davis,
Davis, CA, USA
kwferrara@ucdavis.edu

***Abstract*— Using individual microbubbles (MBs) to image vasculature with a spatial resolution below the diffraction limit has the potential to greatly improve the *in vivo* characterization of healthy and diseased tissue [1-2]. Recent studies have demonstrated a theoretical resolution on the order of microns in stationary tissue using standard imaging arrays [3]. However, the application of this technique to abdominal imaging brings new challenges due to the presence of physiological motion which is far larger than the achievable resolution.**

In this work, single MBs were localized *in vivo* in a rat kidney using a dedicated high frame rate (300 Hz) contrast pulse sequence (CPS) with spatial compounding (-5°, 0°, 5°). A stack of 60000 frames was acquired, providing a B-mode image to track tissue motion and a CPS image to track MB position at each time point. Acquisition was accomplished with a standard imaging array (CL15-7, ATL) driven at 6.9 MHz and a programmable ultrasound system (Verasonics). 3.4 million positions were detected and a density map of the MB positions was obtained after compensation for cardiac motion and changes in kidney position. Blood velocity was also estimated by tracking selected MBs over time.

Keywords—Vascular imaging; super resolution; ultrasound contrast agent; microbubble; kidney imaging.

I. Introduction

Imaging the vasculature on the capillary scale was recently accomplished by tracking the position of individual ultrasound contrast agents acting as point sources [1-2]. This super-localization or super-resolution technique is appealing for characterizing organs or diseases which impact vasculature and blood flow. The theoretically-achievable resolution was demonstrated to be on the order of a few microns for clinical ultrasound frequencies and imaging arrays [3]. However, imaging with sub-diffraction resolution presents challenges *in vivo*, especially for tissues or organs undergoing physiological motion such as respiration. Such motion can then become several orders of magnitude larger than the in plane resolution limit.

The image of the vasculature is constructed by creating a density map of the microbubble (MB) positions after recording a large number of frames (several thousands). The frames are recorded in a few minutes using a high-frame rate system [1] and physiological motion is present in the stack of recorded images for most abdominal imaging applications. Although the high frame rate maximizes the correlation between successive frames, the presence of MBs brings rapid decorrelation in the sequence, especially in highly vascularized organs, which renders accurate motion compensation challenging in acquisitions requiring several minutes.

In this work, we report on super-localization experiments in a rat kidney *in vivo* to evaluate the impact of such motion.

II. Material and method

A. In vivo acquisition

A programmable ultrasound system (Vantage 256, Verasonics, USA) was used to image the vasculature of the left kidney of a female Sprague Dawley rat. The study was approved by the UC Davis Institutional Animal Care and Use Committee. During the experiment, the animal was maintained under anesthesia using 2% isoflurane in oxygen (2 L/min) and body temperature was maintained at 37°C. Imaging was performed with a standard 128-element compact linear array (CL15-7, Phillips ATL, USA).

A contrast pulse sequencing (CPS) mode [4] with spatial compounding was implemented by sending 3 successive single cycle pulses (amplitude ½, -1, ½) with plane waves at 3 different angles (-5°, 0°, 5°); one frame was thus the combination of 9 transmit/receive events. Within a frame, the delay between successive transmissions was minimized; the pulse repetition frequency was 28.5 kHz, and the frame rate was 300 Hz. The center frequency for transmission was 6.9 MHz with a peak negative pressure of 250 kPa for the full amplitude pulse (corresponding to a mechanical index (MI) of ~0.1). These parameters provided an acceptable contrast-to-tissue ratio while limiting MB destruction [5]. A stack of 60000 frames was recorded in 200 s while MBs were continuously injected into the tail vein of the animal with a syringe pump. A total dose of ~3×10^7 non-targeted house-made lipid-shelled MBs (median diameter: 1.3 µm) was injected during the experiment.

Due to the high frame rate, beamforming was performed offline and the raw RF signals were recorded during the experiment. The summation of the RF signals giving the CPS

image (i.e. the summation of the receive matrices for each ½, -1, ½ amplitude pulses) was accomplished prior to beamforming. The availability of the raw RF signals also provided the ability to reconstruct B-mode images at the same time points.

B. Frame selection and microbubble localization

The stack of B-mode images was used to detect motion between successive frames induced by physiological motion. Two-dimensional normalized cross-correlation was calculated in a selected region of interest over the entire stack. Frames acquired during respiratory motion (indicated by a drop in frame to frame correlation) were discarded and the remaining frames were then grouped based on their position in a respiratory cycle such that the frame $F_m(t_i)$ corresponded to the frame at time t_i and localized in the stack between respiratory cycles m and m+1.

Detection of individual MBs was then performed after applying a Gaussian low-pass filter and interpolating to an isotropic 15 µm grid. Positions were recorded based on the profile of the Gaussian shaped point spread function and on the maximum intensity.

Blood velocity was estimated by following MB positions over time. MBs that were tracked over at least 3 successive frames with a position change less than 15 pixels (i.e. 225 µm) between frames were analyzed. The velocity was calculated as the average distance divided by the time interval and the maximum measurable velocity was 67.5 mm/s.

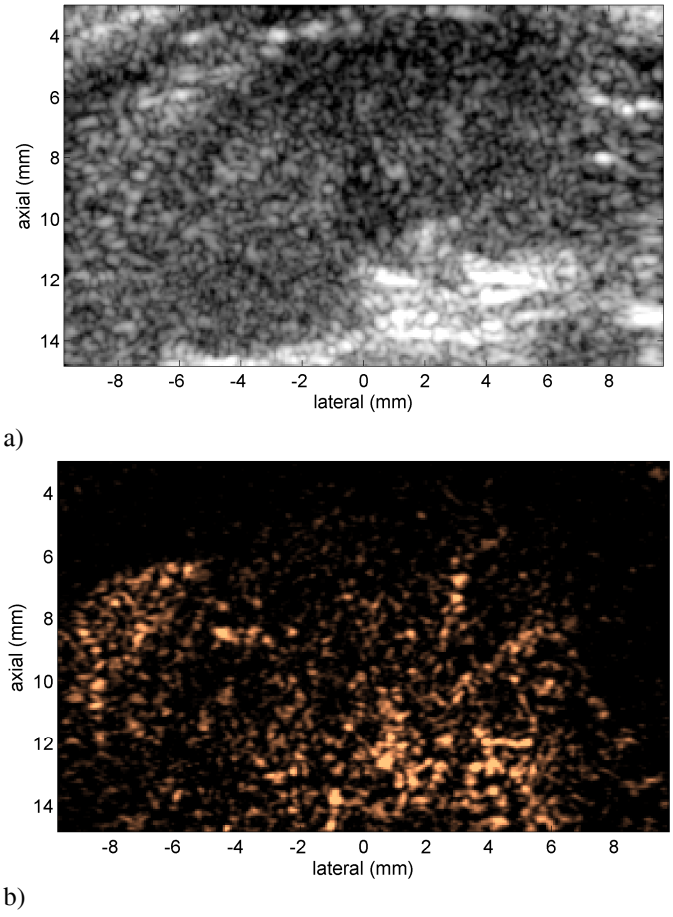

Fig. 1. Both B–mode and CPS images can be extracted from the stack of raw RF-signals. a) B-mode image and b) CPS image of the rat kidney 60 s after starting the continuous injection of MB. The isolated points on the CPS image indicate individual MB.

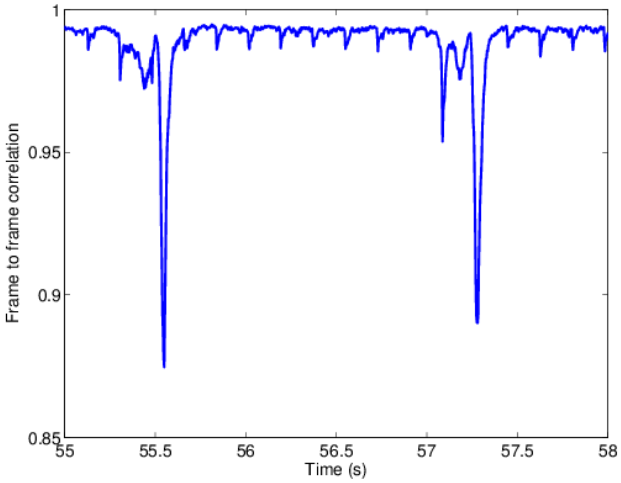

Fig. 2. Magnitude of correlation between successive frames over a small region of interest in the kidney as a function of time. Large decreases in correlation are associated with respiration (here at 55.5 and 57.3 s) while smaller changes are associated with cardiac pulsation. The heart rate in the displayed time window is 336 bpm.

C. Motion compensation

In the sequence that was acquired, two sources of motion affected the kidney position: respiration and cardiac pulsation generated by the abdominal aorta, where respiration was more prominent.

For cardiac pulsation, the displacement of the imaging field was assumed to be uniform and similar for all heartbeats in the sequence to facilitate the compensation process. Displacement was estimated with a 2D cross-correlation block matching algorithm [6]. The resulting compensation was applied to the detected MB positions in the corresponding frames and M density maps were created, each resulting from the detected positions in each of the respiratory cycles.

Lastly, changes in the kidney position between respiratory cycles were estimated assuming rigid kidney motion (translation+rotation). To this end, a least-square algorithm was implemented to estimate motion parameters $\{\Delta x, \Delta z, \theta\}$, where Δx and Δz are the lateral and axial translations, respectively, and θ the rotation, such that the difference between the density map m and a selected reference map was minimized. The final density map was calculated as the average of the motion-compensated M density maps.

III. Results

Images of the kidney from the stack are displayed in Fig. 1. The combination of the B-mode image (Fig. 1a) and the CPS image (Fig. 1b) at each time point was useful to follow

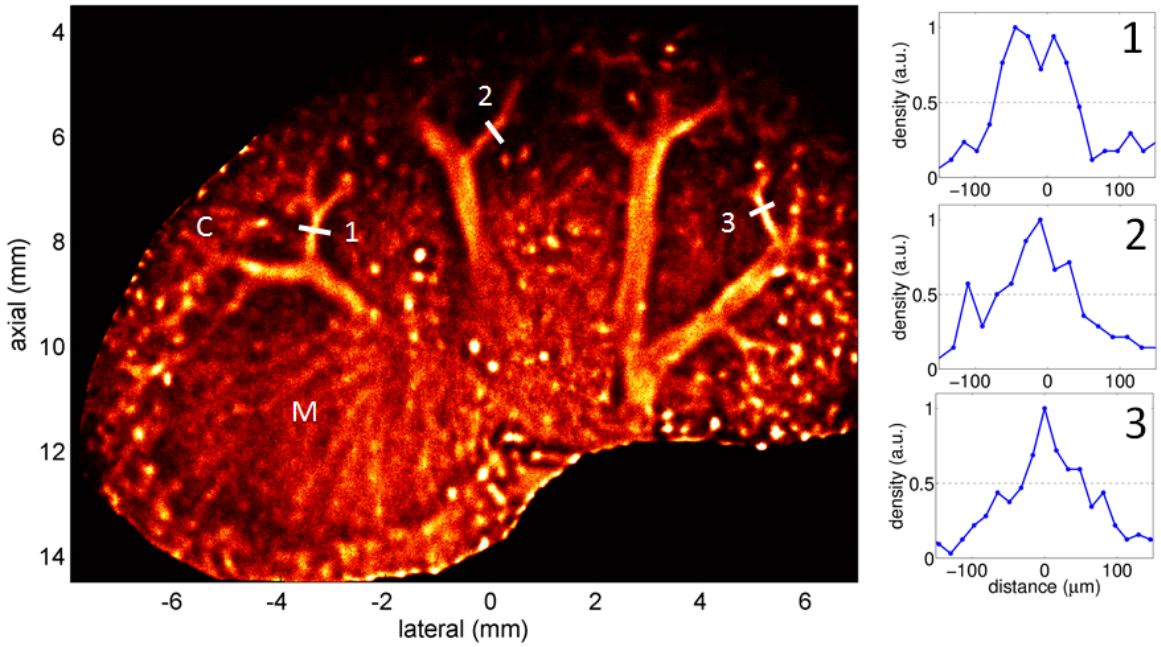

Fig. 3. Density map of the detected MB positions of the rat kidney (left) and profiles of selected vessels (right). A mask was applied to the image to suppress microbubbles detected outside of the kidney. The kidney vascular tree was identified and the cortex (C) and medulla (M) differentiated.

the MBs and track the kidney position.

A. *Processing the stack of frames*

Throughout the sequence, 118 respiratory cycles were recorded (Fig. 2), and 43718 frames remained after the elimination of frames with low correlation. Cardiac-induced motion was also detected with cross-correlation, facilitating estimation of the heartbeat (Fig. 2).

As a result of the high resolution achieved with MB localization, small changes in the kidney position were detected between respiratory cycles.

B. *Super resolved image*

Approximately 3.4 million positions were detected over the stack of images. After motion compensation, combining the MB positions provided a detailed image of the in-plane kidney vasculature as depicted in Fig. 3. Due to the 3D structure of the vasculature, bright spots are apparent on the map and are associated with vessels orientated in the elevation direction (out-of-plane). Consistent with the kidney structure, vascular patterns were differentiated between the cortex and the medulla. Vessels as small as 45 μm were resolved. The elevation resolution of the array, in combination with the dense 3D vessel structure, limited the visualization of individual capillaries (vessels <45 μm). This effect is prominent on the density map in the medulla which stacks the traces of multiple micro vessels.

C. *Blood velocity*

Following MBs over time provided an estimate of the blood velocity as shown in Fig. 4. Higher velocities (>30 mm/s) are demonstrated in the larger vessels, while low velocities (<10 mm/s) are detected in smaller vessels within the medulla. The elevation resolution of the array limits the ability to estimate the velocity in larger vessels where MB signals from both arteries and veins overlap. Hence, a broad range of values (30 to 65 mm/s) is observed in the large vessels.

IV. Conclusion and Discussion

One of the principal opportunities provided by ultrasound contrast agents is their use in mapping microvascular flow rate, a particularly important physiological parameter. In the past, this was accomplished through the use of destruction-replenishment pulse sequences; however, low mechanical index imaging is much more attractive for clinical use. High frame rate imaging protocols, such as the methods described here, can now estimate such flow rates without the need for a high amplitude destructive pulse.

We have previously reported on a method to create sub-resolution images using microbubbles based on transmission at a low frequency and reception at a higher frequency [7]. With this method, broadband microbubble echoes were used to create an image where spatial resolution was independent of the wavelength of transmission. Using current ultrasound transducers, the application of the previous technique to the imaging of deep abdominal organs is limited.

Using MBs to image the vasculature with micron resolution using clinical ultrasound frequencies is a major step in *in vivo* tissue characterization. However, this technique brings new challenges for applications in abdominal imaging when physiological motion is present. In this work, a high frame rate

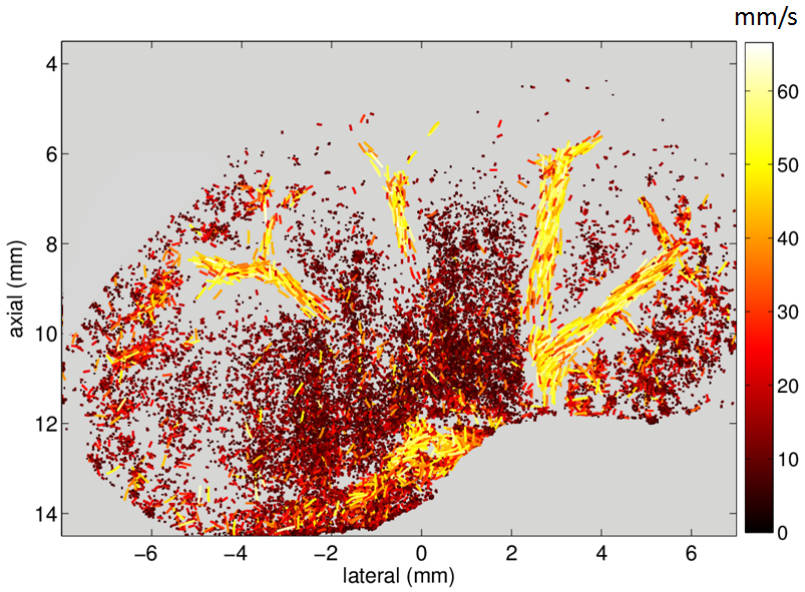

Fig. 4. In-plane velocity map obtained after tracking selected MBs over time. Each segment represents the trajectory of a single MB over at least 3 successive time points. A broad range of velocity amplitudes was detected, with low velocities (<10 mm/s) estimated in the medulla. Most importantly, the techniques applied here provide the opportunity to assay the microvasculature with a low amplitude pulse train.

imaging sequence was developed to localize individual MBs flowing in the kidney of an anesthetized rat under free respiration. Cardiac motion and changes in kidney position due to respiration were compensated and a detailed image of the vasculature and in-plane velocity maps were obtained.

Due to the large number of pulses utilized in the experiment (300 Hz + 3 angles + CPS = 2700 pulses/s), the MI was minimized to limit MB destruction. In this condition, dedicated amplitude-modulation sequences such as CPS have been shown to provide better contrast than frame to frame differentiation for MB imaging [8]. CPS imaging at a high frame rate provides a direct image of the MB position at each time point without the need for high pass spatio-temporal filtering.

Although single MBs are clearly identified in the imaging plane throughout the entire sequence, their position in elevation (out of plane) is more than an order of magnitude less accurate due to the limited elevational focus of the array (0.7 mm at –6 dB, 10 mm away from the array, as measured with a hydrophone). Combined with the dense 3D structure of the kidney vasculature, identification of individual capillaries is difficult. For the same reason, small out-of-plane position changes between successive breaths cannot be fully eliminated. The use of full 2D arrays is appealing for full 3D localization of the MBs.

Future developments aim at improving the SNR from coherent beamforming techniques [9] as well as improving tracking of the individual MBs over time.

ACKNOWLEDGMENT

The authors thank Elisabeth Ingham for her help in preparing MBs during test experiments. This work was supported by NIH grants R01CA112356, R01CA210553, R01CA199658 and R01CA134659.

REFERENCES

[1] C. Errico, J. Pierre, S. Pezet, Y. Desailly, Z. Lenkei, O. Couture, et al., "Ultrafast ultrasound localization microscopy for deep super-resolution vascular imaging," Nature, vol. 527, pp. 499-502.

[2] K. Christensen-Jeffries, R. J. Browning, T. Meng-Xing, C. Dunsby, and R. J. Eckersley, "In Vivo Acoustic Super-Resolution and Super-Resolved Velocity Mapping Using Microbubbles," *Medical Imaging, IEEE Transactions on,* vol. 34, pp. 433-440, 2015.

[3] D. Yann, P. Juliette, C. Olivier, and T. Mickael, "Resolution limits of ultrafast ultrasound localization microscopy," Physics in Medicine and Biology, vol. 60, p. 8723, 2015.

[4] P. J. Phillips, "Contrast pulse sequences (CPS): imaging nonlinear microbubbles," in Ultrasonics Symposium, 2001 IEEE, 2001, pp. 1739-1745 vol.2.

[5] O. Couture, S. Bannouf, G. Montaldo, J.-F. Aubry, M. Fink, and M. Tanter, "Ultrafast Imaging of Ultrasound Contrast Agents," Ultrasound in Medicine & Biology, vol. 35, pp. 1908-1916, 11// 2009.

[6] E. S. Ebbini, "Phase-coupled two-dimensional speckle tracking algorithm," IEEE Transactions on Ultrasonics, Ferroelectrics, and Frequency Control, vol. 53, pp. 972-990, 2006..

[7] D. E. Kruse and K. W. Ferrara, "A new imaging strategy using wideband transient response of ultrasound contrast agents," IEEE Transactions on Ultrasonics, Ferroelectrics, and Frequency Control, vol. 52, pp. 1320-1329, 2005

[8] J. Viti, H. J. Vos, N. d. Jong, F. Guidi, and P. Tortoli, "Detection of Contrast Agents: Plane Wave Versus Focused Transmission," IEEE Trans. on Ultr. Ferr. and Freq. Control, vol. 63, pp. 203-211, 2016.

[9] M. A. L. Bell, J. J. Dahl, and G. E. Trahey, "Resolution and brightness characteristics of short-lag spatial coherence (SLSC) images," IEEE Transactions on Ultrasonics, Ferroelectrics, and Frequency Control, vol. 62, pp. 1265-1276, 2015.